



Auxiliary power through marine waste heat recovery using a CO₂-organic cascading cycle

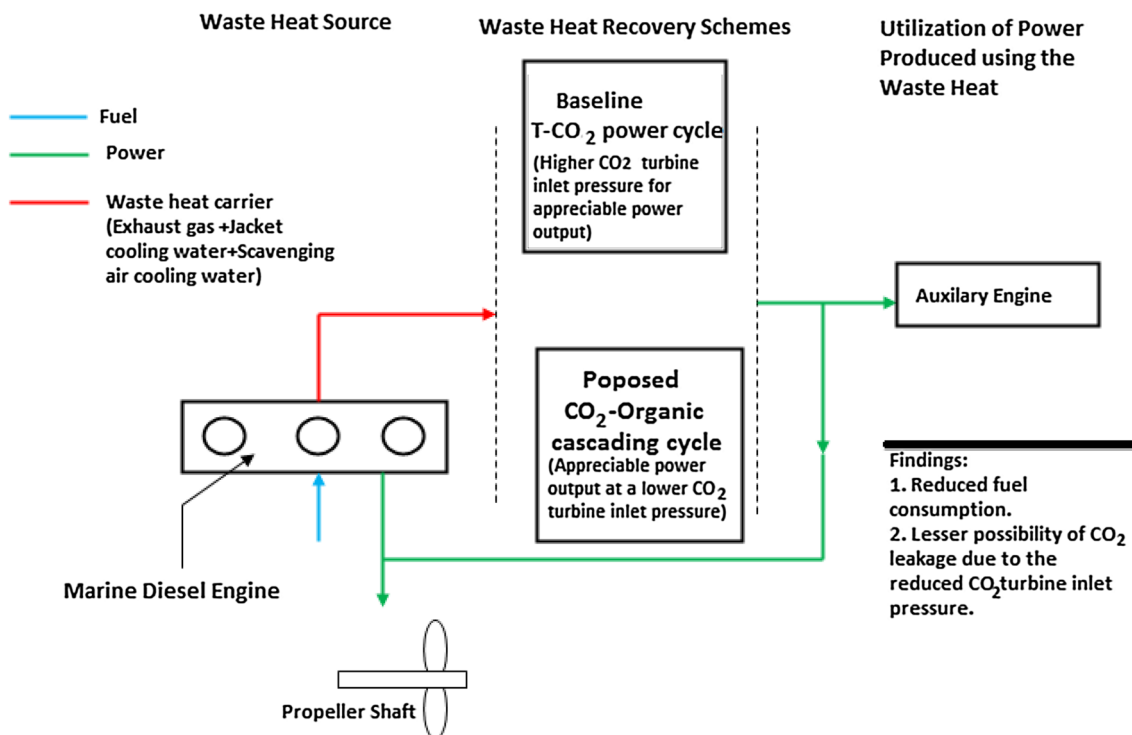
Subha Mondal¹ · Soumitra Datta² · Sudipta De²

Received: 25 June 2019 / Accepted: 28 February 2020 / Published online: 12 March 2020
© Springer-Verlag GmbH Germany, part of Springer Nature 2020

Abstract

An appreciable part of primary energy input to a marine diesel engine is rejected as waste heat. Thus, through marine diesel engine waste heat recovery significant amount of secondary energy can be produced to satisfy the auxiliary power requirement of the marine ship. In present study, a CO₂-organic fluid cascading cycle is considered for the utilization of the waste heat released by the marine diesel engine. R290, R600 and R1233zd (E) are considered as the working fluids of the bottoming cycle for their lower global warming potentials. The analysis revealed that power output of the cascading cycle is comparable to that of the baseline transcritical CO₂ power cycle. However, for similar power output, operating pressure in the flue gas-CO₂ heat recovery unit of the transcritical CO₂ power cycle is significantly higher compared to that of the cascading cycle. Thus, possible leakage due to very high operating pressure of a conventional CO₂ power cycle can be addressed by using the cascading system. Bare module costs per unit power output of cascading cycles are also significantly smaller. It is also apparent from the study that the marine diesel engine waste heat recovery through the CO₂-organic cascading cycle would lead to 8–9.5% annual fuel saving. Reduced fuel consumption will also result in lesser CO₂ emission from the marine ship.

Graphic abstract



Keywords Marine diesel engine · Waste heat · CO₂ power cycle · CO₂-organic cascading · Bare module cost

List of symbols

C_P^0	Purchase cost of equipment (\$)
c_p	Specific heat (kJ kg ⁻¹ K)
C_{BM}	Bare module cost (\$)
d_i	Inside tube diameter (m)
G	Mass flux (kg m ⁻² s ⁻¹)
g	Acceleration due to gravity (ms ⁻²)
h	Enthalpy (kJ kg ⁻¹ K ⁻¹)
k	Thermal conductivity (W m ⁻¹ K ⁻¹)
M	Molecular weight of working fluid (g mol ⁻¹)
m	Mass flow rate (kg s ⁻¹)
Nu	Nusselt number
Pr	Prandtl number
P	Pressure (MPa)
Q	Heat transfer (kW)
Re	Reynolds number
s	Entropy (kJ kg ⁻¹ K ⁻¹)
T	Temperature (°C)
$T_{g,i}$	Exhaust gas inlet temperature (°C)
$T_{g,o}$	Exhaust gas outlet temperature (°C)
ΔT	Logarithmic mean temperature difference (°C)
U	Overall heat transfer coefficient of heat exchanger (W m ⁻² K ⁻¹)
$W_{t,tur}$	Power output of the turbine of topping cycle (kW)
$W_{b,tur}$	Power output of the turbine of bottoming cycle (kW)
$W_{t,pump}$	Power consumed by pump of topping cycle (kW)
$W_{b,pump}$	Power consumed by pump of bottoming cycle (kW)
$W_{t,NET}$	Net power output of topping cycle (MW)
$W_{b,NET}$	Net power output of bottoming cycle (MW)
W_{CASCAD}	Power output of cascade cycle (MW)
X	Equipment type
Y	Capacity or size parameter of equipment (m ² or kW)

Greek symbols

α	Convective heat transfer coefficient (W m ⁻² K ⁻¹)
μ	Dynamic viscosity (Pa s)
ρ	Density

Subscripts

b	Bottoming cycle
con	Condensation, condenser
cw	Cooling water
cyl	Cylinder cooling water
exh	Exhaust gas

exp	Expander
i	Inside, inlet
j	Section
o	Outside
r	Organic working fluid for bottoming cycle
sca	Scavenging air cooling water
t	Topping cycle
tur	Turbine

Abbreviations

BMC	Bare module cost
COFHURU	CO ₂ -organic fluid heat recovery unit
CEPCI	Chemical engineering plant cost index
FGCHRURU	Flue gas CO ₂ heat recovery unit
GWP	Global warming potential
ODP	Ozone depletion potential
ORC	Organic Rankine cycle
TRC	Transcritical Rankine cycle

Introduction

About three hundred million metric tons of fossil fuel is consumed by ocean-going ships in a year (Corbett and Koehler 2003). Thus, consumption of fossil fuels and emission from these ships are issues of great concern. The cost associated with marine transport is also increasing steadily due to escalating fuel prices. Recently, it was reported by Mondal and De (2020) that conversion of readily available low and medium grade heat into power and other energy utilities would reduce fossil fuel consumption and greenhouse gas emission simultaneously. Appreciable amount of thermal energy is carried away by exhaust flue gas, scavenging air cooling water and jacket cooling water of any marine diesel engine. This waste heat may be utilized to produce some secondary energy. Thus, there is a great scope in a marine diesel engine to reduce both fuel consumption and associated emission by cutting down fuel consumption by adopting an efficient waste heat recovery scheme.

Recent studies indicated that organic Rankine cycle is one of the emerging technologies to generate power from low and medium grade heat. Braimakis and Karellas (2018) analyzed the performance of regenerative organic Rankine cycles using hot pressurized water as the heat source. Baik et al. (2013) reported that while utilizing low-temperature geothermal heat, the transcritical ORC with R125 yielded higher power output compared to the power outputs of subcritical ORCs using R134a, R245fa

and R152a as working fluids. Saleh et al. (2007) pointed out that in an ORC a supercritical working fluid should be used to maximize the heat transfer from the low-temperature heat carrier.

Organic flash cycle (OFC) is also emerging as a possible technology for low-grade waste heat utilization due to the absence of pinch limitation in the heat recovery unit. The study conducted by Ho et al. (2012) revealed that the utilization efficiency of an organic flash cycle (OFC) was comparable to that of a basic ORC. Mondal and De (2017a) reported that an OFC would be economically preferred over a T-CO₂ power cycle for producing power from low-grade waste heat of the flue gas, free from SO₂. To reduce irreversibility of the OFC, Mondal and De (2017b) proposed to replace the low-pressure throttle valve of the OFC by an ejector that entrained the working fluid exiting the evaporator of a refrigeration cycle. Mondal et al. (2018) also incorporated an ejector in an OFC to increase the turbine power output. Mondal and De (2019) showed that the possibility of accidental flame propagation with R600 could be reduced appreciably by using a mixture of R245fa and R600 as the working fluid of an OFC. The GWP of the mixture was also smaller than the GWP of pure R245fa.

CO₂ is a nonflammable, non-toxic and environment friendly working fluid. Thus, CO₂-based power cycle would be preferred for low-grade heat recovery. Guo et al. (2010) showed that power output of a low-grade heat-driven T-CO₂ power cycle had been 3–7% higher compared to an organic Rankine cycle using R245fa as the working fluid. Mondal and De (2015a) proposed a regenerative T-CO₂ power cycle that utilized the heat of the turbine bleed gas to preheat the CO₂ stream entering the heat recovery unit. Mondal and De (2015b) revealed that specific power output and 2nd law efficiency of a low-grade heat-driven supercritical CO₂ power cycle could be enhanced by increasing the number of compression stages along with intercooling.

In recent time, substantial research is going on marine diesel engine waste heat recovery. Song et al. (2015) showed that an ORC can be driven economically by the waste heat released by a marine diesel engine. Yang and Yeh (2015) demonstrated that while recovering waste heat from a large marine diesel engine, the ORC with R1234yf would exhibit superior thermo-economic performance compared to those of the ORCs using R1234ze, R152a, R600a and R245fa as working fluids. Yang (2016) conducted the optimization of a marine diesel engine waste heat recovery system to select the best possible working fluids for the transcritical ORC. According to his analysis, R236fa appeared as the best performing working fluids out of six considered working fluids. Yang (2018) also evaluated the payback period for ORC-based marine engine waste heat recovery system that utilized mixtures of different working fluids instead of a pure working fluid. Yang and Yeh (2017) proposed a

new parameter, namely “net power output index” to evaluate the economic performance of the marine diesel engine exhaust-driven transcritical organic Rankine cycle (TORC). In many of the recent studies, CO₂-based power cycles were considered for engine waste heat recovery mainly due to nonflammable, non-toxic and environment friendly nature of CO₂. CO₂ is also readily available at a lower cost. It is also preferred for engine waste heat recovery as it is chemically stable even at higher temperature (Song et al. 2018). Shi et al. (2017) experimentally evaluated the performance of an engine waste heat-driven T-CO₂ power cycle. Chen et al. (2005) reported that the engine waste heat could be used as the input to a CO₂-based power cycle to reduce the fuel consumption of a vehicle.

Most of the previous studies presented marine diesel engine waste heat recovery by using either organic Rankine cycle or CO₂-based power cycles. It should be noted that operating pressure in the heat recovery unit of the CO₂-based power cycle should be significantly high to ensure an acceptable thermal efficiency. Most of the low GWP organic fluids are either flammable or commercially unavailable. Thus, the selection of suitable working fluid for waste heat recovery is a challenging task. By using a CO₂-organic cascading cycle, the high operating pressure in the heat recovery unit of the CO₂-based power cycle can be decreased. The risk of flame propagation with the cascading cycle will also be less as the requisite mass of organic working fluid is significantly smaller for the cascading system. Thus, in the present study, cascading between a CO₂ power cycle and a transcritical ORC is considered for the marine diesel engine waste heat recovery to address the above issues. The cycle is designated as CO₂-organic cascading cycle, with CO₂ cycle as the topping one. R600, R290 and R1233zd (E) are considered as the different alternative working fluid of the bottoming cycle of the cascading due to their lower GWP. The proposed system is analyzed thermodynamically considering a regenerative T-CO₂ power cycle as the baseline system.

In the proposed waste heat recovery scheme, to maximize the thermal efficiency, CO₂ is heated to a temperature (~270 °C) which is closest to the inlet temperature (~290 °C) of the engine exhaust gas. The mass flow rate of CO₂ is estimated from the energy balance of the flue gas-CO₂ heat recovery unit (FGCHRU). It should be noted that the entire mass of jacket cooling water is utilized to preheat the CO₂ before entering the FGCHRU. At a lower operating pressure of the FGCHRU (i.e., < 13 MPa), heat available with the mass of jacket cooling water is not sufficient to preheat CO₂ from pump exit condition to the inlet condition of the FGCHRU. Thus, for lower pressures of the FGCHRU, a small mass of scavenging air cooling water is directed through another heater to preheat the CO₂ stream from pump exit condition to the inlet condition of the heater recovering the heat of the jacket cooling water. Some mass

Table 1 Waste heat from a large marine diesel engine (Yang 2016)

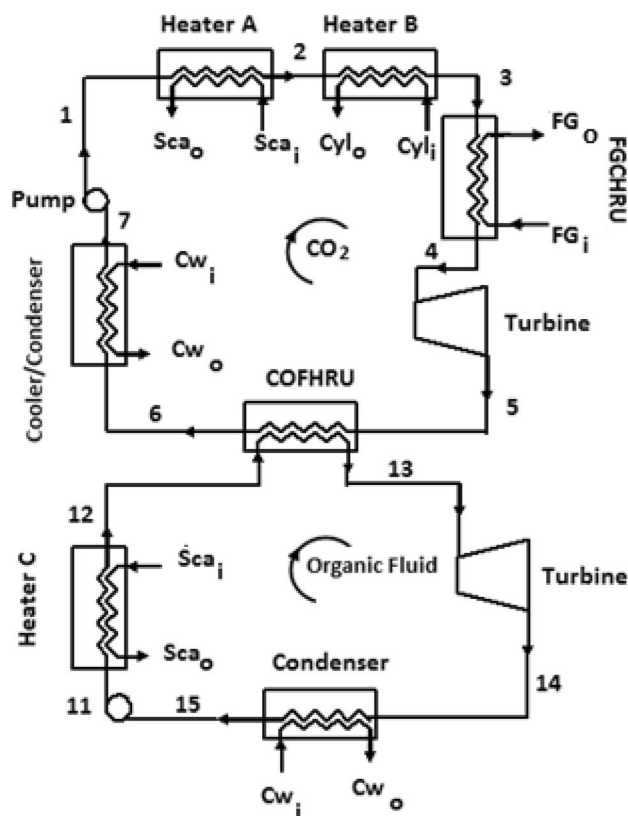
Waste heat source	Mass flow rate (kg/s)	Inlet temperature (°C)	Minimal exit temperature (°C)
Exhaust gas	148.51	290	138
Cylinder jacket cooling water	158	90	74
Scavenge air cooling water	162.5	76	36

of scavenging air cooling water is also utilized to preheat the organic fluid before entering into the CO₂-organic fluid heat recovery unit (COFHUR). Even after these distributions, heat carried with a certain mass fraction of the scavenging air cooling water remains unutilized. In short, in the present study, flowing mass of cylinder jacket cooling water as well as scavenging air cooling water are split into different streams and directed through three different preheaters to maximize the heat recovery from these sources.

System description

In the present work, exhaust gas, cylinder jacket cooling water and scavenging air cooling water of a large marine diesel engine are considered as waste heat sources. Heat content along with the inlet and outlet temperature of the above mentioned streams are summarized in Table 1 (Yang 2016).

Layout of proposed CO₂-organic fluid cascading cycle, utilizing waste heat from a marine engine is presented in Fig. 1. Figure 2a, b is T-S diagrams for the topping transcritical CO₂ cycle and bottoming transcritical ORC, respectively. The sequence of waste heat recovery by the CO₂ is according to the available temperature. CO₂ stream exiting the pump at state-1 recovers heat from scavenging air cooling water, jacket cooling water and exhaust flue gas of a large marine diesel engine in Heater-A (i.e., process 1–2), Heater-B (i.e., process 2–3) and flue gas-CO₂ heat recovery unit (FGCHRU) (i.e., process 3–4), respectively. The intention of the present study is to heat the CO₂ stream close to the flue gas inlet temperature to ensure the higher thermal efficiency. Thus the CO₂ stream is heated to 270 °C by the heat of exhaust flue gas stream. Mass flow rate of CO₂ stream is estimated from the energy balance of the FGCHRU. The CO₂ mass at state-4 enters the expander (i.e., the turbine) to produce the power output. The temperature of CO₂ stream at the exit of the turbine (i.e., state-5) is appreciably high. Thus, this CO₂ is cooled (process 5–6) in a CO₂-organic fluid heat recovery unit (COFHUR) by exchanging heat to any one of the three selected organic fluids. The organic fluid exiting the COFHUR (at state-13) also expands (i.e., process 13–14) in a turbine to produce some power output. The organic fluid also recovers heat

**Fig. 1** Layout of the CO₂-organic cascading cycle

from the scavenging air cooling water in heaters C (i.e., process 11–12) before entering the COFHUR. Organic fluid mass flow rate is estimated from the energy balance of the COFHUR.

It should be noted that at higher operating pressures (i.e., above 13 MPa) of the FGCHRU CO₂, mass flow rate reduces appreciably and available mass of jacket cooling water is slightly higher than the mass required to preheat the CO₂ from pump exit condition (i.e., state 1) to the inlet condition of the FGCHRU (i.e., state 3). Thus, Heater-A is to be removed from the system layout if the pressure in the FGCHRU is above 13 MPa. Otherwise, both heaters (i.e., Heater-A and Heater-B) are required.

Selection of suitable working fluid for the bottoming organic cycle is critical as use of the chlorofluorocarbon (CFCS) and most of the hydro-chlorofluorocarbons (HCFCs) are restricted due to either ozone-depleting nature or higher values of GWP. HFCs are to be phased out soon according to Kigali amendment to the Montreal protocol. In present study, two hydrocarbons (R290, R600) and one HFO (R1233zd (E)) refrigerant are considered as the working fluid of the bottoming cycle due to lower values of GWP as listed in Table 2. As turbine exit temperature of topping CO₂ cycle varies between 190 and 235 °C, the bottoming organic cycle can be heated in transcritical mode.

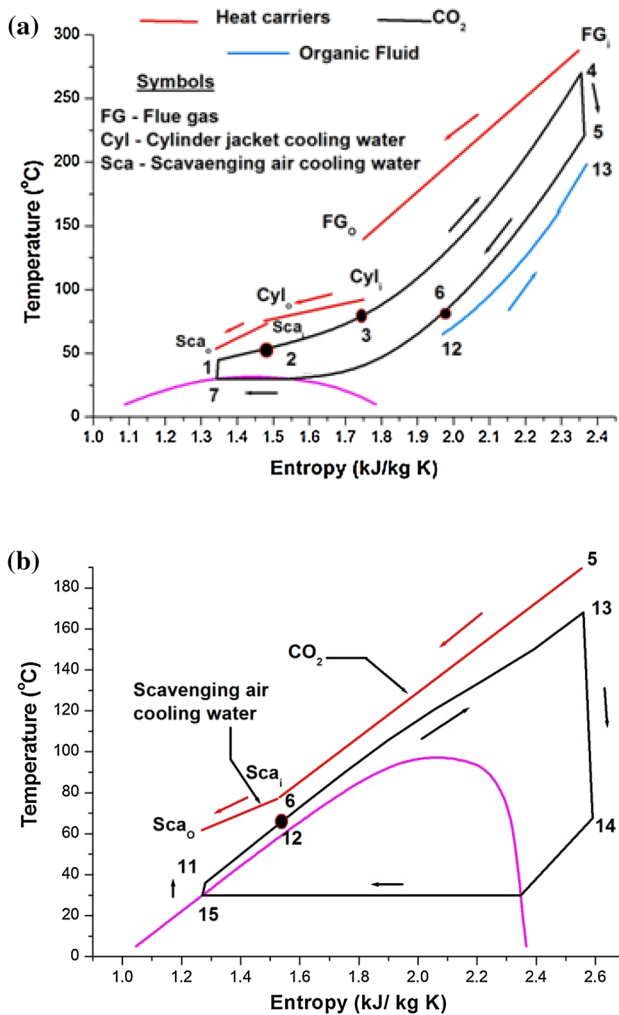


Fig. 2 T-S diagram for **a** topping CO₂ cycle of the cascading. **b** Bottoming transcritical ORC of the cascading

Layout of the engine waste heat-driven baseline T-CO₂ power cycle is presented in Fig. 3. In the baseline T-CO₂ power cycle, CO₂ stream exiting the jacket cooling water is heated in the regenerator (i.e., process 13–14) by the heat of the CO₂ stream exiting the turbine. CO₂ mass flow rate for the baseline T-CO₂ power cycle is also estimated from the energy balance of the FGCHRU. For better representation

of operating conditions, terminal temperature differences in different heat recovery units are presented in Table 3.

Mathematical modeling

In initial part of the mathematical modeling, from the mass and energy balance of each of the equipment, equations are developed to represent the energetic performances of the waste heat recovery scheme. Thermodynamic and transport properties of various working fluids are evaluated using REFPROP-9.1 (Lemmon et al. 2013). During the modeling, following assumptions are considered to simplify the analysis:

1. All the equipments are steady flow devices.
2. Turbine isentropic efficiency is 90%.
3. Isentropic efficiencies of the pump as well as the compressor are assumed to be 85% each.
4. Ambient condition is specified by 100 kPa and 20 °C.
5. Maximum permissible flue gas velocity is 15 m/s.
6. All heat exchangers are assumed to have shell-and-tube configuration with multi pass arrangement.
7. During heat exchanger design flue gas thermo-physical properties are assumed to be same as air.

Thermodynamic modeling

Mass flow rate CO₂ through the topping cycle can be evaluated from the energy balance of the FGCHRU as follows:

$$m_{CO2} = \frac{m_g c_{Pg} (T_{g,i} - T_{g,o})}{(h_4 - h_3)} \tag{1}$$

Mass flow rate organic working fluid through the bottoming cycle can be evaluated from the energy balance of the COFHRU as presented in Eq. 2:

$$m_f = \frac{m_{CO2} (h_5 - h_6)}{(h_{13} - h_{12})} \tag{2}$$

Power outputs from topping cycle turbine and bottoming cycle turbine are estimated in Eqs. 3 and 4, respectively.

Table 2 Properties of selected working fluids for bottoming cycle (Calm and Hourahan 2011; Yang et al. 2018)

Properties	R290	R1233zd (E)	R600
Critical temperature (°C)	96.68	166.45	151.98
Critical pressure (MPa)	4.2471	3.6237	3.7960
ODP	0	0	0
GWP(100 years) (kg/kg of CO ₂)	20	7	20
ASHRAE safety category	A3 (highly flammable)	A1 (nonflammable)	A3 (highly flammable)

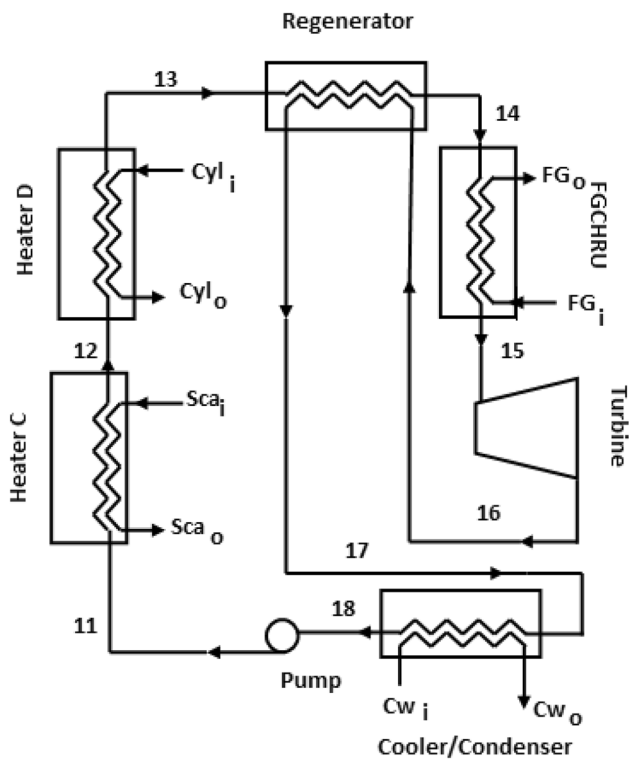


Fig. 3 Layout of baseline Regenerative T-CO₂ power cycle

Table 3 Terminal temperature differences in HRUs

Cycle	Heat recovery unit	Δt_{LTE} (°C)	Δt_{HTE} (°C)
CO ₂ -organic cascading	FGCHRU	48	20
	Heater-A	10	Variable
	Heater-B	Variable	10
	Heater-C	30	10
	COFHRU	10	20
Baseline regenerative T-CO ₂	FGCHRU	10	20
	Heater-C	10	Variable
	Heater-D	Variable	10
	Regenerator	Variable	Variable

$$W_{t,tur} = m_{CO_2}(h_4 - h_5) \tag{3}$$

$$W_{b,tur} = m_r(h_{13} - h_{14}) \tag{4}$$

Equations 5 and 6 are representing pump power inputs of the topping cycle and the bottoming cycle, respectively.

$$W_{t,pump} = m_{CO_2}(h_1 - h_7) \tag{5}$$

$$W_{b,pump} = m_r(h_{11} - h_{15}) \tag{6}$$

Now, net power outputs of the topping cycle as well as the bottoming cycle are evaluated as follows:

$$W_{t,NET} = |W_{t,tur}| - |W_{t,pump}| \tag{7}$$

$$W_{b,NET} = |W_{b,tur}| - |W_{b,pump}| \tag{8}$$

Now, power output of the cascading cycle

$$W_{Cascade} = W_{t,NET} + W_{b,NET} \tag{9}$$

Heat exchanger area estimation

Heat exchangers are divided in “N” number of subsections for taking care of varying transport property of working fluids with varying temperature. Enthalpy drops across each of the subsections are assumed to be equal. Now area of any one of the subsections can be evaluated as follows:

$$A_{exh,j} = \frac{Q_{exh,j}}{U_{exh,j}F\Delta T_{mean,exh,j}} \tag{10}$$

In Eq. 10, $\Delta T_{mean,exh,j}$ is LMTD (logarithmic mean temperature difference) for the counter flow arrangement and F is correction factor to take care of multi passes. Elemental heat duty of Eq. 10 can be estimated by Eq. 11.

$$Q_{exh,j} = \frac{m_{WF} |h_i - h_o|}{N} \tag{11}$$

In Eq. 11, h_i and h_o are enthalpies of working fluid in inlet and exit of the heat exchanger, respectively.

Overall, heat transfer coefficient of each of the heat exchanger element can be expressed as

$$U_{exh,j} = \frac{1}{1/\alpha_{tube} + 1/\alpha_{shell}} \tag{12}$$

α_{tube} and α_{shell} are tube side and shell side convective heat transfer coefficients, respectively. Various correlations considered for convective heat transfer coefficients are summarized in Table 4.

Bare module cost estimation

In order to estimate the cost of the equipment for preliminary design, the cost equations proposed by Turton et al. (2013) are employed. Equation used for the purchased cost of individual equipment (C_p^0) at ambient operating pressure and using carbon steel (CS) construction is as follows:

$$\log_{10} C_p^0 = K_1 + K_2 \log_{10} Z + K_3 (\log_{10} Z)^2 \tag{13}$$

Table 4 Correlations for estimation of convective heat transfer coefficient (Piro et al. 2004; Incropera and Dewitt 2002; Kreith and Bohn 1993; Cengel and Boles 2006)

Equation of heat transfer coefficient	Fluid	Phase	Heat exchanger
$Nu = \left[\frac{\left(\frac{f_b}{8}\right) Re_r Pr_r}{(f_b/8)^{0.5} \left(Pr_r^{\frac{2}{3}} - 1\right) + 1.07} \right] \left(\frac{C_{pav}}{C_{pv}}\right) \left(\frac{k_b}{k_{wall}}\right) \left(\frac{\mu_b}{\mu_{wall}}\right)$ <p> $0.5 \leq Pr \leq 2000$ $3 \times 10^3 \leq Re \leq 5 \times 10^6$ </p>	Working fluid	Supercritical	FGCHRU COFHUR Heaters A–D
$Nu = \left[\frac{\left(\frac{f_b}{8}\right) Re_r Pr_r}{(f_b/8)^{0.5} \left(Pr_r^{\frac{2}{3}} - 1\right) + 1.07} \right]$		CO ₂ vapor	COFHUR CO ₂ cooler
$Nu = 0.05 Re_{eq}^{0.8} Pr_{satliq}^{0.33}$ $Re_{eq} = Re_{vap} \frac{\mu_{satvap}}{\mu_{satliq}} \left(\frac{\rho_{satliq}}{\rho_{satvap}}\right)^{0.5} + Re_{liq}$ $Re_{liq} = G(1-x) \frac{d_i}{\mu_{satliq}}$ $Re_{vap} = Gx \frac{d_i}{\mu_{satvap}}$		Two-phase CO ₂	CO ₂ condenser
$Nu = 0.0131 Re^{0.883} Pr^{0.36}$ <p> $4.5 \times 10^5 \leq Re \leq 7 \times 10^6$ </p>	Exhaust Gas	Organic fluid vapor	Condenser
$Nu = 0.729 \left(\frac{g \rho_l (\rho_l - \rho_g) D_o^3 i_{fg}'}{\mu_l K_s (T_{sat} - T_{wall})}\right)^{1/4}$		Two phase organic fluid	Condenser
$Nu = 0.71 Re^{0.5} Pr^{0.36} \left(\frac{Pr}{Pr_{wall}}\right)^{0.25}$ <p> $1000 \leq Re \leq 2 \times 10^5$ </p>	Exhaust Gas	Gas	FGCHRU
$Nu = 0.023 Re^{0.8} Pr^{0.3}$ <p> $Re > 10^4$ $0.7 \leq Pr < 160$ </p>	Jacket cooling water, scavenging air cooling water, cooling water	Liquid	Heaters A, B, C, D, condenser

Table 5 Equipment cost parameters (Turton et al. 2013)

Equipments	Performance parameters (Z)	K ₁	K ₂	K ₃	B ₁	B ₂	F _M	C ₁	C ₂	C ₃
FGCHRU	A _{exh} (m ²)	4.3247	−0.303	0.1634	1.63	1.66	1.4	0.0388	−0.11272	0.08183
Heaters A, B, C, D	A _{sca} , A _{cyl} (m ²)									
Condenser	A _{con} (m ²)									
COFHUR	A _{reg} (m ²)	4.3247	−0.303	0.1634	1.63	1.66	1.4	−0.395	0.3957	−0.00226
Pump	W _{pump} (kW)	3.3892	0.0536	0.1538	1.89	1.35	−0.3935	−0.395	0.3957	−0.00226
Turbine	W _{Tur} (kW)	2.7051	1.4398	−0.1776	0	1	3.4	0	0	0

where Z is the parameter for capacity and size of the equipment as provided in Table 5. K₁, K₂, K₃ are the constants, as shown in Table 5. Since the equipments rarely operate at ambient pressure, pressure factor F_p is used to take care of elevated operating pressure. The bare module cost for shell-and-tube heat exchangers and pump is given by

$$C_{BM} = C_p^0 (B_1 + B_2 F_p F_M) = C_p^0 F_{BM} \tag{14}$$

Bare module cost of turbine is expressed as

$$C_{BM} = C_p^0 F_p F_{BM} \tag{15}$$

In these equations, F_p ; F_M and F_{BM} are pressure factor, material factor and bare module factor, respectively, constants. B_1 and B_2 are constants as presented Table 5 (Turton et al. 2013). F_p can be estimate from following equation

$$\log_{10} F_p = C_1 + C_2 \log_{10} (10P - 1) + C_3 (\log_{10} (10P - 1))^2 \quad (16)$$

C_1 , C_2 and C_3 are constants whose values are also provided in Table 5. In Eq. 16, P is the operating pressure in MPa. Subsequently the total cost of the equipments is obtained by adding the cost of individual equipments used in the system as shown below

$$C_{\text{Tot}} = \sum (C_{\text{BM,eq}}) * \frac{\text{CEPCI}_{\text{current year}}}{\text{CEPCI}_{2001}} \quad (17)$$

In Eq. 17, CEPCI is the chemical engineering plant cost index, taking the effect of time on purchased equipment cost into account.

Results and discussion

In the present study, a cascading between T-CO₂ power cycle and Organic Rankine cycle is considered for the recovery of waste heat rejected by a large marine diesel engine. Results are presented by considering a regenerative T-CO₂ power cycle as the baseline one.

The mass flow of CO₂ for the cascading cycle is determined from the energy balance between CO₂ and exhaust gas in the flue gas-CO₂ HRU (FGCHRU). It can be seen from Fig. 4a that the mass flow rate of CO₂ decreases with an increase in FGCHRU pressure. This can be easily explained from Fig. 4b. It is observed in Fig. 4b that with an increase in pressure of the FGCHRU, both h_3 and h_4 decreases (refer to Fig. 2a). However, difference between h_4 and h_3 increases with an increase in pressure of the FGCHRU. Thus, heated mass of CO₂ reduces as heat released by flue gas is constant.

Power output of the topping cycle of the cascading increases with an increase in FGCHRU pressure as shown in Fig. 5. The total power is directly proportional to product of mass and the specific work output. Although the mass flow rate decreases, it is overcompensated by specific work output and thereby increasing the power.

With an increase in topping cycle turbine inlet pressure, CO₂ mass flow rate decreases as already presented in Fig. 4a. Temperature of CO₂ exiting the turbine of the topping cycle also reduces with an increase in FGCHRU pressure as shown in Fig. 6. Lower turbine exit temperature of the topping cycle also results in lower turbine inlet temperature for the bottoming ORC. Thus, total heat available for heating the organic fluid of bottoming cycle as well as efficiency of the bottoming cycle reduces. Due to reduction in heat input as well

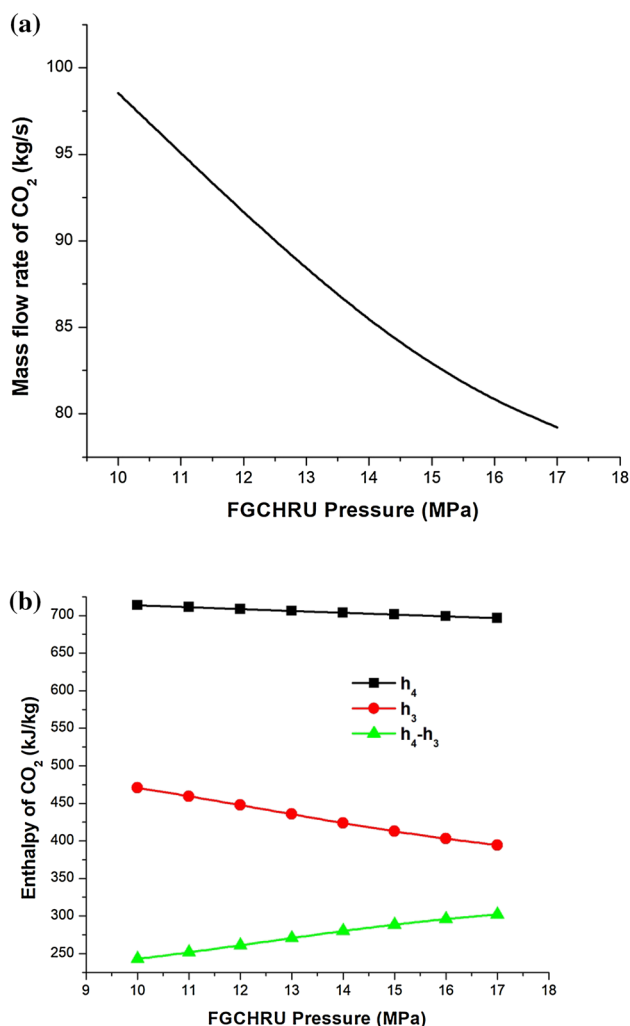


Fig. 4 **a** CO₂ mass flow rate of the topping CO₂ power cycle versus FGCHRU pressure. **b** State point enthalpy variation with varying pressure in FGCHRU

as thermal efficiency, power output of the bottoming cycle decreases with an increase in FGCHRU pressure as shown in Fig. 7.

The total power output of the cascading cycle ultimately increases with an increase in FGCHRU pressure as shown in Fig. 8. It is important to note that improvement achieved in total power output of CO₂-organic cascading cycle becomes negligible above a certain value of FGCHRU pressure. It is also observed in Fig. 8 that for a specified working fluid and FGCHRU pressure, total power output of the cascading cycle increases with an increase in bottoming cycle turbine inlet pressure. However, above a certain value of bottoming cycle turbine inlet pressure, this improvement is almost negligible. Thus, for a specified pressure of FGCHRU, there exists a turbine inlet pressure of the bottoming cycle above which no appreciable improvement in power output of the cascading cycle occurs.

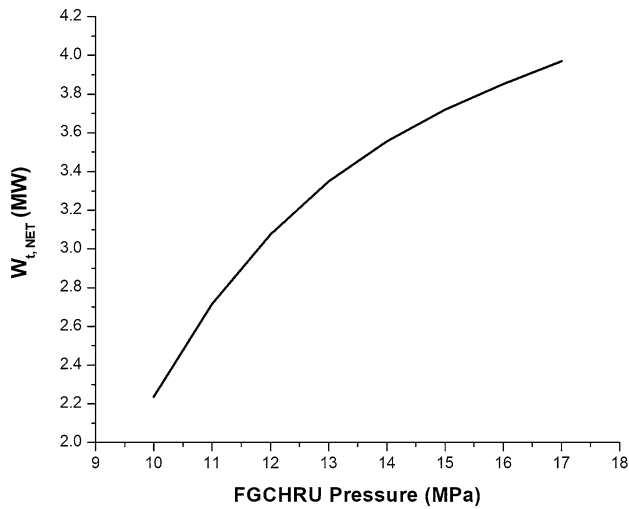


Fig. 5 Power output of the topping CO₂ power cycle versus FGCHRU pressure

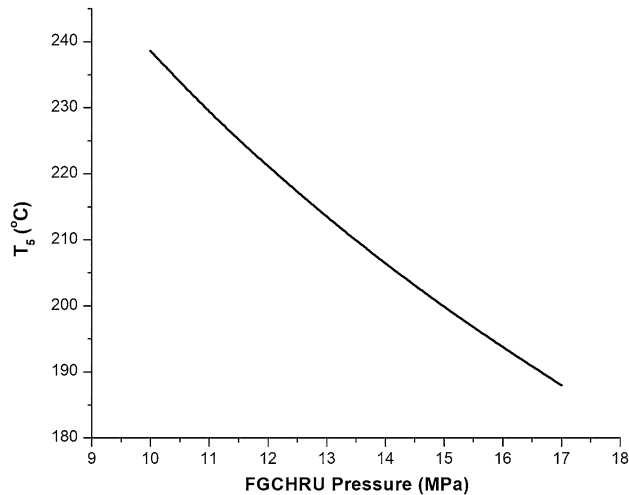


Fig. 6 CO₂ turbine exit temperature (T_5) versus FGCHRU pressure

In Fig. 9, power outputs of the cascading cycle are compared with the power outputs of the baseline cycle (i.e., the regenerative T-CO₂ power cycle) for varying FGCHRU pressure. R290, R600 and R1233zd (E) are working fluids considered for the bottoming cycle of the CO₂-Organic cascading cycle. For all cascading systems, power outputs are considered at the bottoming cycle turbine inlet pressure above which power output of a cascading cycle becomes almost insensitive to the varying bottoming cycle turbine inlet pressure. The total power output of the cascading cycle increases with an increase in pressure of the FGCHRU and reaches to a peak if R1233zd (E) or R600 is used as the working fluid of the bottoming cycle. For R290, above a certain value of the FGCHRU pressure, the

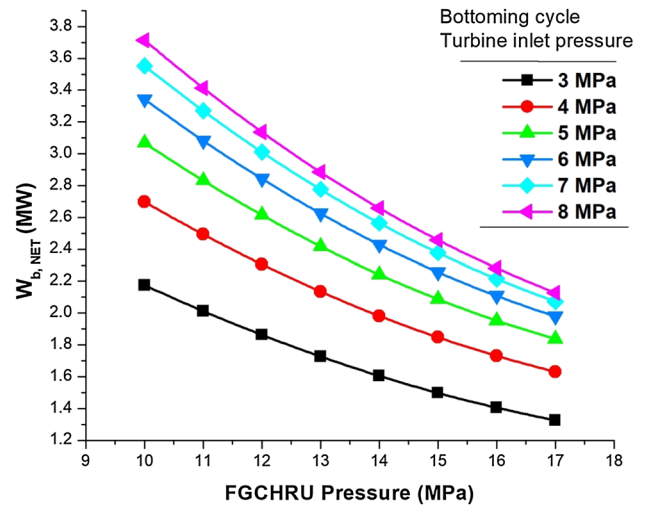


Fig. 7 Power output of the bottoming ORC with R290 versus FGCHRU pressure

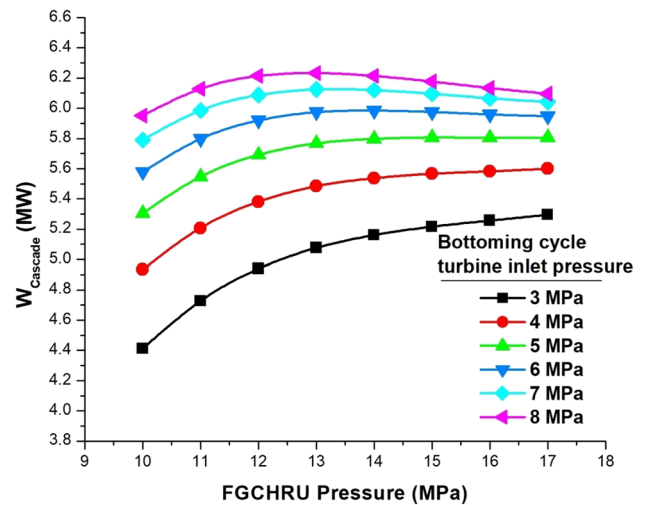


Fig. 8 Power output of the CO₂-R290 cascading cycle versus FGCHRU pressure

variation of cascading cycle power output is negligible. It is also observed that for lower values of FGCHRU pressure (< 15 MPa), the cascading cycle can yield appreciably higher power output compared to that of the baseline regenerative T-CO₂ power cycle with all three selected working fluids of the bottoming cycle. The cascading cycle yields the highest power output if R1233zd (E) is used as the working fluid of the bottoming cycle of cascading. As pressure in the FGCHRU is increased, the power output of the baseline cycle increases sharply and becomes comparable to that of the cascading cycles as the pressure in the FGCHRU reaches close to 16 MPa.

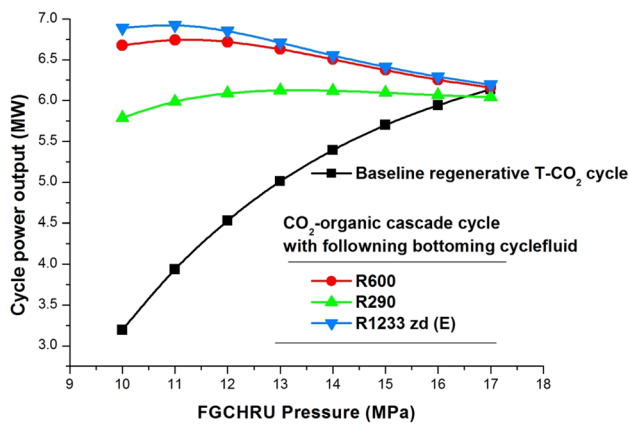


Fig. 9 Comparison of power output of cascading cycle with that of the baseline T-CO₂ cycle

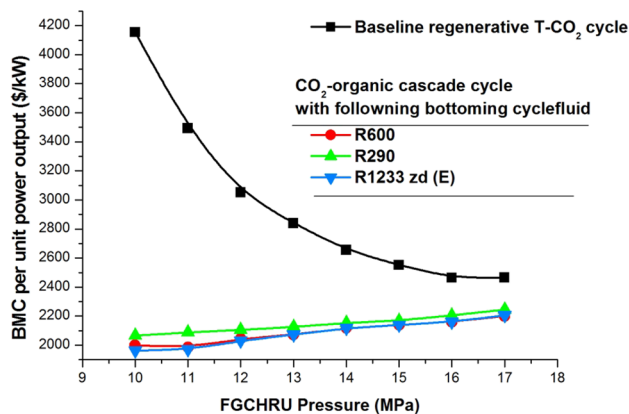


Fig. 10 Comparison of BMC of cascading cycle with that of the baseline T-CO₂ cycle

Effects of varying FGCHRU pressure on bare module cost per unit power output is presented in Fig. 10. It is observed in Fig. 10 that at a lower FGCHRU pressure BMC per unit power is appreciably higher for the baseline T-CO₂ power cycle. However, BMC per unit power output reduces sharply as elevated pressure is ensured in the FGCHRU. It should be noted that though the total BMC of the base line cycle increases with an increasing FGCHRU pressure, BMC per unit power sharply reduces with the increasing pressure of FGCHRU due to steady rise in cycle power output. Beyond a certain value of the FGCHRU pressure, reduction achieved in BMC per unit power output of the baseline cycle is negligible.

It is further observed in Fig. 10 that BMC per unit power output of all the cascading cycles are appreciably smaller compared to the baseline cycle, especially at lower pressures of the FGCHRU. This is due to higher power outputs of cascading cycles at lower operating pressures of FGCHRUs. However, BMC per unit power of the

cascading cycle increases slowly with increasing pressure of the FGCHRU.

For similar heat carriers, the power output of the present waste heat recovery scheme is appreciably higher compared to that was produced by the waste heat recovery system proposed by Yang (2016). This is occurring because in the present study the thermal efficiency is maximized by heating CO₂ closer to the engine exhaust gas and the heat recovery from jacket cooling water and scavenging air cooling water also maximized by distributing their mass flow to three different heaters. On the other hand, Yang (2016) tried to minimize the costing parameters while designing the waste heat recovery system.

In Fig. 11, 1st law efficiency of the proposed waste heat-driven cascade system is compared with that of a regenerative T-CO₂ power cycle without heat recovery. While estimating 1st law efficiency of the regenerative T-CO₂ power cycle, regenerator heat duty is maximized by maintaining 10 °C terminal temperature difference in the low temperature end of the CO₂ regenerator. It is observed in Fig. 11, that for close to 10 MPa CO₂ turbine inlet pressure, 1st law efficiencies of both cycles are almost equal. However, for higher turbine inlet pressure, 1st law efficiency of the regenerative T-CO₂ power cycle without heat recovery is appreciably higher compared to that of the proposed waste heat-driven cascade system. It is important to note that though 1st law efficiency of the regenerative T-CO₂ power cycle without heat recovery is appreciably high; it is not suitable for marine diesel engine waste heat recovery. This is because the temperature of CO₂ exiting the regenerator is so high that heat available with jacket cooling water and scavenging air cooling water cannot be recovered. Thus, due to smaller heat input power output of the regenerative T-CO₂ power

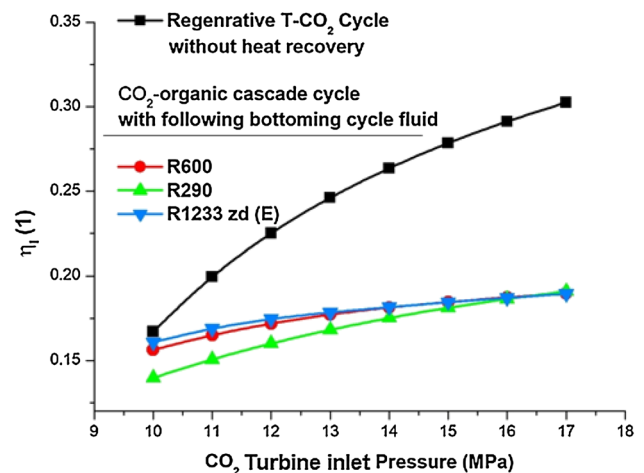


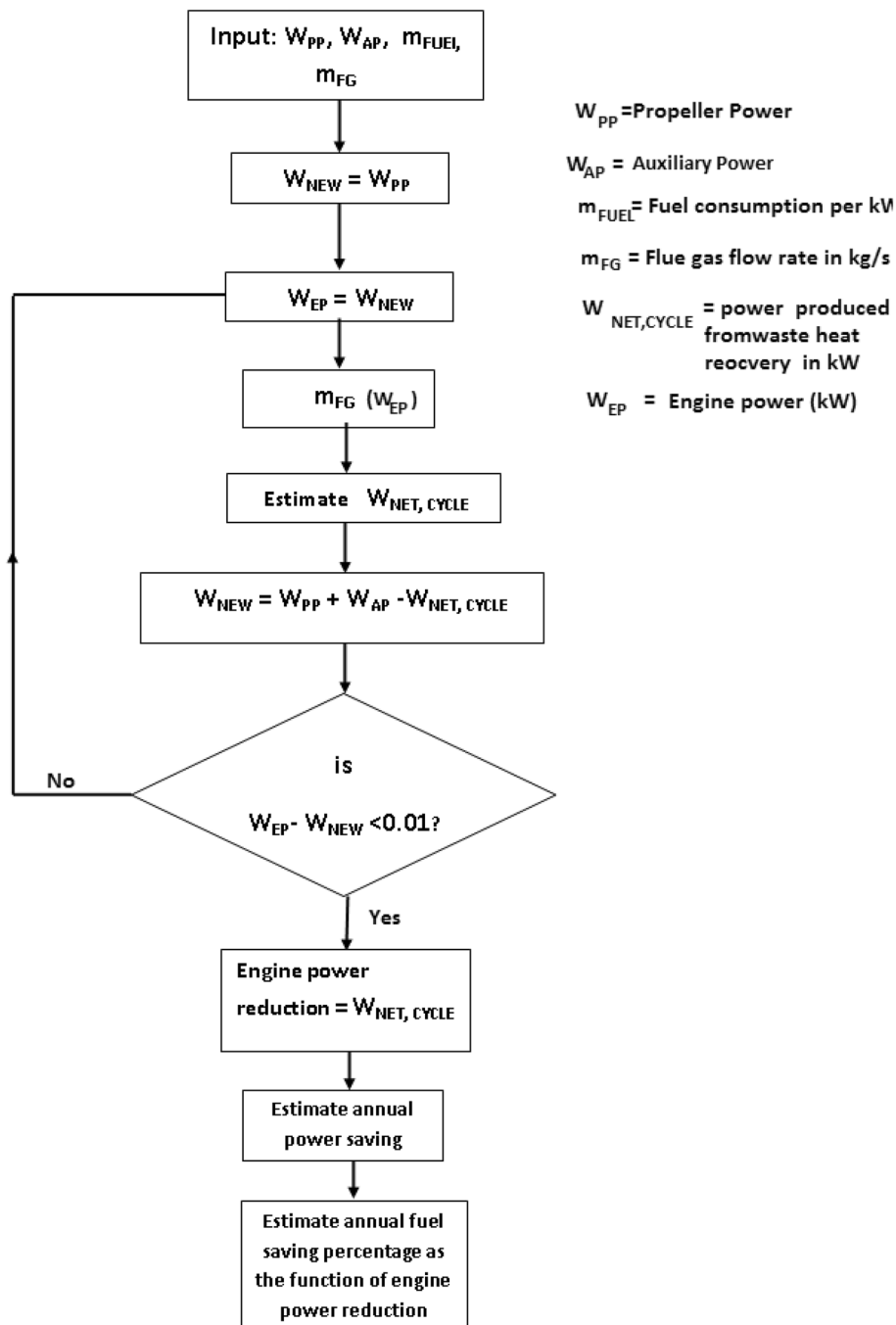
Fig. 11 Comparison between 1st law efficiency of the waste heat-driven cascade cycle and that of the regenerative T-CO₂ cycle without heat recovery

cycle will be appreciably small if regenerator heat duty is maximized.

It should be noted that the auxiliary power requirement of a ship may be assumed to be 5% of the total power output of a marine diesel engine (Malley et al. 2015). Thus, the additional power produced from waste heat recovery can be utilized to supply the auxiliary power. The power produced by the waste heat recovery scheme may be higher to some extent compared to the auxiliary power requirement of the ship. In this situation, after catering the auxiliary power,

the remaining power of the waste heat recovery system may be utilized to reduce propeller engine power requirement. However, this would affect output of the waste heat recovery unit as available waste heat would also reduce. Thus, if power output of the waste heat recovery unit is higher compared to the power requirement of the auxiliary unit, fuel savings due to the incorporation of waste heat recovery scheme can be estimated through an iterative calculation as shown in Fig. 12. During this calculation, fuel consumption is assumed to be 0.167 kg/kW-h and annual operation

Fig. 12 Methodology for the estimation of fuel saving



hour is assumed to be 7200 h. Waste heat released by the engine supplying the propeller power is only considered for the waste heat recovery.

The annual fuel savings is closely related with the additional power produced by the proposed waste heat recovery scheme. The more the power produced, the greater is the fuel saving. The percentage of oil saved is plotted for CO₂-organic fluid cascade system and regenerative T-CO₂ cycle operating at FGCHRU pressures of 10 MPa (Fig. 13a) and 16 MPa (Fig. 13b), respectively. It is observed that at lower operating pressure of 10 MPa, the CO₂-R1233zd (E) cascading cycle can save 9.53% of fuel annually while the same is significantly lower in regenerative T-CO₂ at 4.62%. The annual fuel saving percentage improves significantly for regenerative T-CO₂ cycle when the FGCHRU pressure is increased. The annual fuel savings for regenerative T-CO₂ cycle at 16 MPa is 8.25% which is marginally lower than the CO₂-organic cascade cycle. It is interesting to note from Fig. 14 that the annual fuel savings of CO₂-organic cascade cycle does not vary significantly with FGCHRU pressures but that of regenerative T-CO₂ cycle improves significantly, owing to higher power output at higher pressure. However, operating at lower pressure is

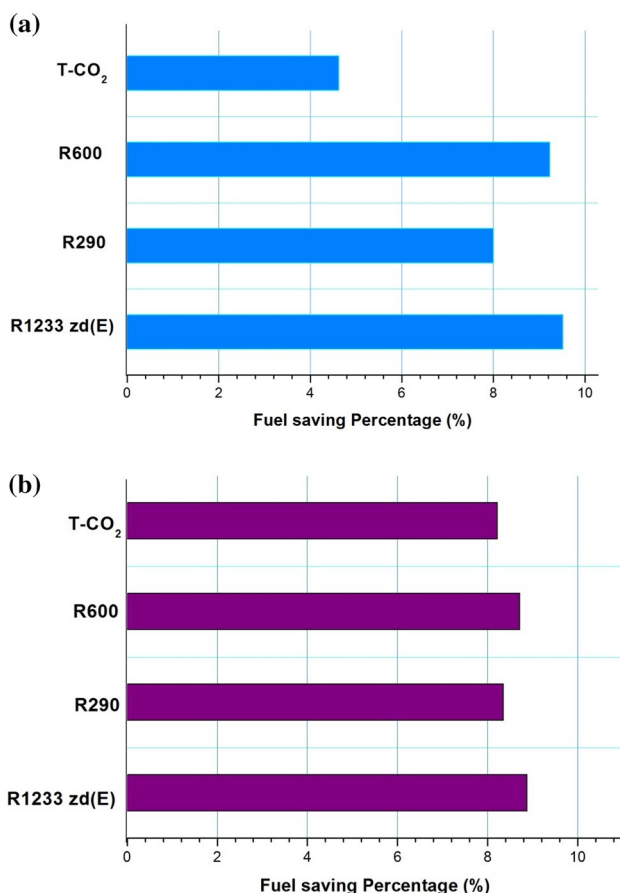


Fig. 13 Annual fuel saving due to waste heat recovery at **a** 10 MPa, **b** 16 MPa pressure in the FGCHRU

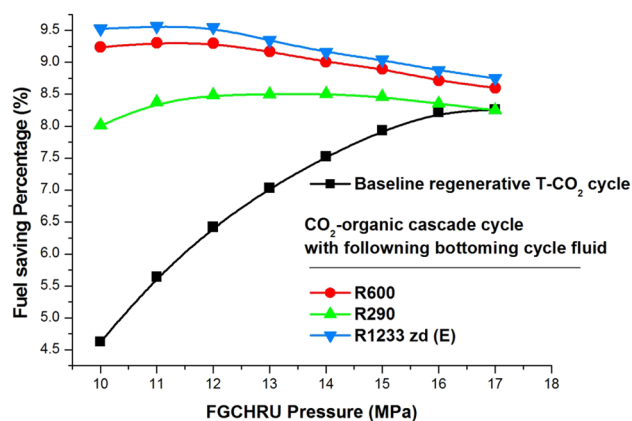


Fig. 14 Annual fuel saving versus FGCHRU pressure

always better from capital investment as well as operational simplicity. Hence, cascaded cycle will provide better overall performance than T-CO₂ cycle with better oil saving operating at lower pressure.

It is also necessary to compare the power output of the cascading cycle with that of a regenerative transcritical organic Rankine cycle to select the best possible waste heat recovery scheme for a marine diesel engine. In Fig. 15a, the power output of the regenerative ORC with R290 is compared with that of the CO₂-R290 cascading cycle. Initially, the power output of the regenerative ORC increases with increasing operating pressure in the organic fluid HRU. Then the power output decreases due to the reduced heat duty of the regenerator. A slightly increasing trend is observed further as specific turbine power output increases with the elevated pressure in organic fluid HRU. It is observed in Fig. 15a that the power output of a regenerative ORC with R290 is higher compared to the power produced by a CO₂-R290 cascading cycle. For the cascading cycle, pressure in the FGCHRU is taken to be 12 MPa or less to avoid the leakage of CO₂ from the piping joint.

It is clear from Fig. 15b that the mass flow rate of the R290 for each MW power output of the regenerative ORC is appreciably higher compared to that of the CO₂-R290 cascading cycle yielding the same power output. Thus, the chance of the accidental and uncontrolled flame propagation would be reduced appreciably by using a CO₂-organic cascading cycle for the marine diesel engine waste heat recovery as mass of flammable working fluid to be handled reduces appreciably.

Conclusions

In the present study, a cascading between a T-CO₂ power cycle and an organic Rankine cycle is considered for the marine diesel engine waste heat recovery. R290, R600 and

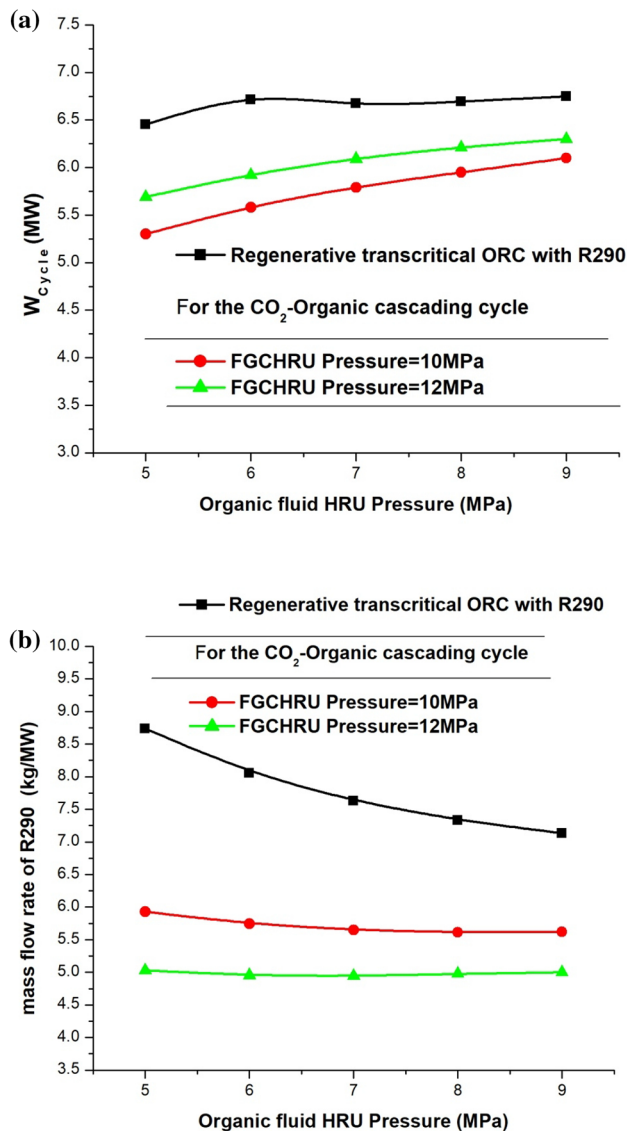


Fig. 15 **a** Comparison between of power output of regenerative ORC with R290 and that of CO₂-R290 cascading. **b** Comparison of mass flow rate of R290 in regenerative ORC to that of in CO₂-R290 cascading cycle

R1233zd (E) are selected as the working fluids of the bottoming cycle considering their lower GWPs. The outcome of the study can be summarized as follows:

- By using the marine diesel engine waste heat, a CO₂-organic cascading cycle yields good power output even at 10 MPa pressure in the flue gas-CO₂ heat recovery unit (FGCHRU). For producing a comparable power output, the pressure in the FGCHRU of the baseline regenerative T-CO₂ power cycle should be close to 16 MPa.
- The bare module cost for producing each kW power output appears to be smaller for the cascading cycle com-

pared to that of the baseline regenerative transcritical CO₂ power cycle.

- In present study, R1233zd (E) appears as the best performing working fluid, as the cascading cycle that is using R1233zd (E) as bottoming cycle fluid yields highest power and lowest BMC per kW. Waste heat recovery through CO₂- R1233zd (E) cascading cycle would reduce annual fuel consumption by 9.53%.

In summary, marine diesel engine waste heat recovery through the CO₂-organic cascading cycle would produce a less adverse effect on the environment as it would reduce marine CO₂ emission by cutting down the fuel consumption.

References

- Baik Y-J, Kim M, Chang K-C, Lee Y-S, Yoon H-K (2013) A comparative study of power optimization in low-temperature geothermal heat source driven R125 transcritical cycle and HFC organic Rankine cycles. *Renew Energy* 54:78–84
- Braimakis K, Karellas S (2018) Energetic optimization of regenerative Organic Rankine Cycle (ORC) configurations. *Energy Convers Manag* 159:353–370
- Calm JM, Hourahan GC (2011) Physical, safety, and environmental data for current and alternative refrigerants. In: Conference physical, safety, and environmental data for current and alternative refrigerants, Prague, Czech Republic, pp 21–26
- Cengel YA, Boles MA (2006) *Thermodynamics: an engineering approach*, 5th edn. McGrawHill, New York
- Chen Y, Lundqvist P, Platell P (2005) Theoretical research of carbon dioxide power cycle application in automobile industry to reduce vehicle's fuel consumption. *Appl Therm Eng* 25:2041–2053
- Corbett JJ, Koehler HW (2003) Updated emissions from ocean shipping. *J Geophys Res* 108(D20):4650. <https://doi.org/10.1029/2003JD003751>
- Guo T, Wang HX, Zhang SJ (2010) Comparative analysis of CO₂-based transcritical Rankine cycle and HFC245fa-based subcritical organic Rankine cycle using low temperature geothermal source. *Sci China* 53:1638–1646
- Ho T, Samuel SM, Greif R (2012) Comparison of the Organic Flash Cycle (OFC) to other advanced vapor cycles for intermediate and high temperature waste heat reclamation and solar thermal energy. *Energy* 42:213–223
- Incropera FP, Dewitt DP (2002) *Fundamentals of heat and mass transfer*, 5th edn. Wiley, New York
- Kreith F, Bohn MS (1993) *Principles of heat transfer*, 5th edn. West Publishing Company, New York
- Lemmon EW, Huber ML, McLinden MO (2013) NIST standard reference database 23: reference fluid thermodynamic and transport properties—REFPROP, version 9.1. National Institute of Standards and Technology, Standard Reference Data Program, Gaithersburg
- Malley S, Walsh K, Hasen A, Bratvold D, Ratafia-Brown J (2015) Marine fuel choice for ocean going vessels within emission control areas. Energy Information Administration
- Mondal S, De S (2015a) Transcritical CO₂ power cycle—effects of regenerative heating using turbine bleed gas at intermediate pressure. *Energy* 87:95–103
- Mondal S, De S (2015b) CO₂ based power cycle with multi-stage compression and intercooling for low temperature waste heat recovery. *Energy* 90:1132–1143

- Mondal S, De S (2017a) Power by waste heat recovery from low temperature industrial flue gas by Organic Flash Cycle (OFC) and transcritical-CO₂ power cycle: a comparative study through combined thermodynamic and economic analysis. *Energy* 121:832–840
- Mondal S, De S (2017b) Ejector based organic flash combined power and refrigeration cycle (OFC&RC)—a scheme for low grade waste heat recovery. *Energy* 134:638–648
- Mondal S, De S (2019) Waste heat recovery through organic flash cycle (OFC) using R245fa–R600 mixture as the working fluid. *Clean Technol Environ Policy* 21:1575–1586
- Mondal S, De S (2020) Power and other energy utilities from low grade waste heat—novel technologies to reduce carbon footprint. *Encycl Renew Sustain Mater* 3:667–677
- Mondal S, Alam S, De S (2018) Performance assessment of a low grade waste heat driven organic flash cycle (OFC) with ejector. *Energy* 163:849–862
- Pioro IL, Khartabil HF, Duffey RB (2004) Heat transfer to supercritical fluids flowing in channels—empirical correlations (survey). *Nucl Eng Des* 230:69–91
- Saleh B, Koglbauer G, Wendland M, Fischer J (2007) Working fluids for low-temperature organic Rankine cycles. *Energy* 32:1210–1221
- Shi L, Shu G, Tian H, Chang L, Huang G, Chen T (2017) Experimental investigations on a CO₂-based Transcritical Power Cycle (CTPC) for waste heat recovery of diesel engine. *Energy Procedia* 129:95
- Song J, Song Y, Gu C (2015) Thermodynamic analysis and performance optimization of an Organic Rankine Cycle (ORC) waste heat recovery system for marine diesel engines. *Energy* 82:976–985
- Song J, Li X, Ren X, Gu C (2018) Performance improvement of a pre-heating supercritical CO₂ (S-CO₂) cycle based system for engine waste heat recovery. *Energy Convers Manag* 161:225–233
- Turton R, Bailie RC, Whiting WB (2013) Analysis, synthesis and design of chemical processes, 4th edn. Prentice Hall PTR, New Jersey
- Yang M (2016) Optimizations of the waste heat recovery system for a large marine diesel engine based on transcritical Rankine cycle. *Energy* 113:1109–1124
- Yang M (2018) Payback period investigation of the organic Rankine cycle with mixed working fluids to recover waste heat from the exhaust gas of a large marine diesel engine. *Energy Convers Manag* 162:189–202
- Yang M, Yeh R (2015) Thermo-economic optimization of an organic Rankine cycle system for large marine diesel engine waste heat recovery. *Energy* 82:256–268
- Yang M, Yeh R (2017) Economic research of the transcritical Rankine cycle systems to recover waste heat from the marine medium-speed diesel engine. *Appl Therm Eng* 114:1343–1354
- Yang J, Sun Z, Yu B, Chen J (2018) Experimental comparison and optimization guidance of R1233zd (E) as a drop-in replacement to R245fa for organic Rankine cycle application. *Appl Therm Eng* 141:10–19

Publisher's Note Springer Nature remains neutral with regard to jurisdictional claims in published maps and institutional affiliations.

Affiliations

Subha Mondal¹ · Soumitra Datta² · Sudipta De²

✉ Sudipta De
de_sudipta@rediffmail.com

¹ Department of Mechanical Engineering, Aliah University, Kolkata 700160, India

² Department of Mechanical Engineering, Jadavpur University, Kolkata 700032, India